Decahedra and icosahedra everywhere: The anomalous crystallization of Au and other metals at the nanoscale

Blake Rogers[1], Alexander Lehr[1], J. Jesús Velazquez-Salazar[1], Robert Whetten[1,4], Ruben Mendoza-Cruz[2], Lourdes Bazan-Diaz[2], Daniel Bahena-Uribe[3] and Miguel José Yacaman[1,4]*

[1]Applied Physics and Materials science department. Northern Arizona University, Flagstaff, AZ 86011, USA

[2]Instituto de Investigaciones en Materiales, Universidad Nacional Autónoma de México. Circuito Exterior, Ciudad Universitaria, Ciudad de México, México, 04510.

[3]Laboratorio de Microscopia Electrónica Cinvestav–IPN, México City México

[4]¡MIRA! institute Northern Arizona University

*Corresponding Author: miguel.yacaman@nau.edu

Keywords: decahedral and icosahedral nanoparticles, nanotechnology, electron microscopy, nanoalloys

Abstract

Throughout history objects with five-fold symmetry have been a popular topic of interest for artists, philosophers, and scientists. This may be because five-fold symmetry is very conspicuous in nature. In the case of crystals, five-fold rotational symmetry is mathematically forbidden, and macroscopic crystals exhibiting five-fold symmetry have never been shown to exist. Nevertheless, in the nanoworld we often find nanoparticles with decahedral and icosahedral shapes that have an overall pseudo five-fold symmetry. These structures are observed at many length scales from 1nm up to 1μm. In this review we discuss several reasons for the stability of five-fold nanoparticles. These include the formation of twin boundaries, surface reconstruction faceting and other factors.

Figure 1: Examples of five-fold symmetry in nature.

1) Introduction

Objects with five-fold symmetry are very common in nature. We can see it in flowers, seashells and other objects[1] (as illustrated in **Figure 1**). It is known that in plants five-fold arrangements increase light harvesting and therefore photosynthesis[1]. In the case of classical crystals, it is established that in a bulk crystal the rotational symmetry 360/n can only have n = 1, 2, 3, 4 and 6 which results in repeatable rotation angle values. Five-fold symmetry, where n=5 is not allowed in classical crystals. We can explain this if the rotational symmetry reflects the shape of a polygon. We can fill the space with squares, triangles, and hexagons, but we cannot do it with pentagons. Suppose that we want to fabricate a decahedron from a pack of regular tetrahedra, and the rotation angle of the decahedron is 72^0 or $360^0/5$. The result is show in **Figure 2** and we end up with a gap. To close the gap strain on the tetrahedral units is necessary. It becomes clear that decahedral structures are not likely to be stable if crystal growth continues after their formation, and in bulk crystals, decahedral structures have been never observed. The discovery of quasicrystals indicates that true rotational five-fold symmetry can exists in a bulk solid however the price to pay is a lack of translational symmetry[2].

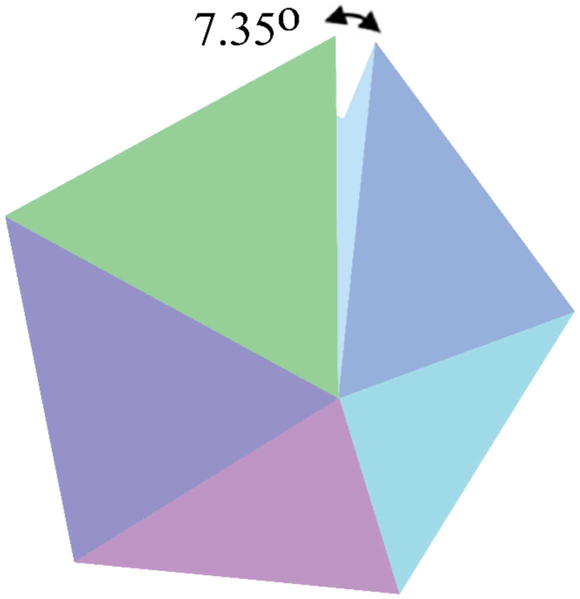

Figure 2: Image showing five-fold symmetry and the gap introduced due to the integer value of five not being allowed for rotational symmetry. Reprinted (adapted) with permission from Casillas et al., A New Mechanism of Stabilization of Large Decahedral Nanoparticles. Journal of Physical Chemistry C, 2012. 116(15): p. 8844-8848. Copyright 2012 American Chemical Society.

In the nanoworld however, decahedral structures are easily formed from sizes of a few nanometers up to several micrometers. Five-fold structures have been observed in different cases such as metals, alloys, semiconductors[3], carbon in fullerenes, diamond[4] and many other compounds. A large proportion of viruses have an icosahedral capsid[5-7]. In the case of carbon, the five-fold structure can be easily understood since all the atomic bonds are satisfied, but the case for metals is much more intriguing.

In this paper we will review the main mechanisms that explain the unanticipated stability of decahedral and icosahedral single metal nanoparticles. Decahedral and icosahedral structures formed at different sizes are shown in **Figure 3**. To study metal nanoparticles, transmission electron microscopy (TEM) has been a fundamental technique for understanding nanoparticle structure. Initially dark field images were used but the resolution of the TEM was limited[8-10]. An important advancement was the use of high-resolution machines in the late 70's[11]. The introduction of image and probe aberration correctors two decades ago produced a quantum change in our understanding of metallic nanoparticles. The generalized use of High Angle Annular Dark Field (HAADF) on the scanning transmission mode (STEM) increased our understanding of atomic positions and therefore strain.

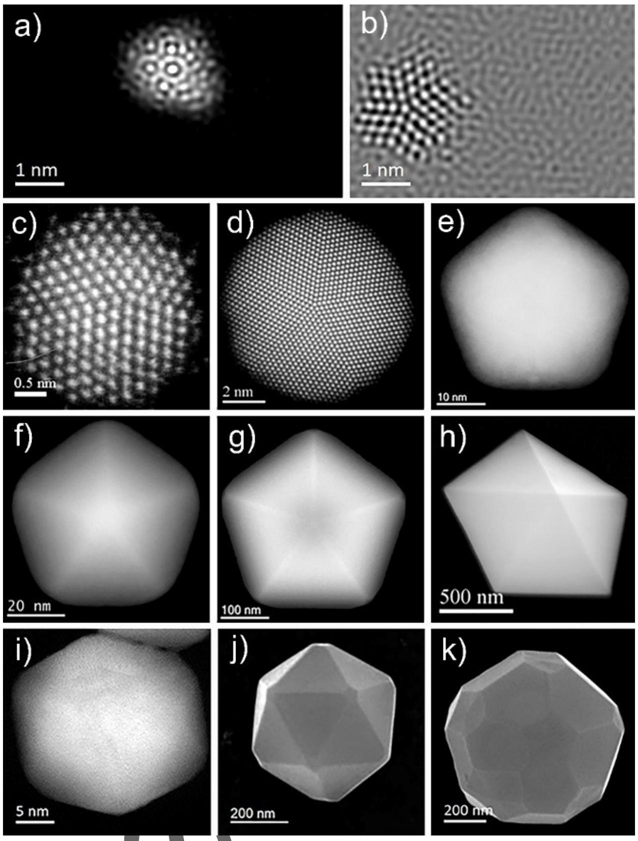

Figure 3: Examples of decahedral and icosahedral structures shown at different sizes. The five-fold symmetry can be seen in all the structures from the a) cluster size all the way to h) the microparticle size. Reprinted (adapted) with permission from Casillas et al., A New Mechanism of Stabilization of Large Decahedral Nanoparticles. Journal of Physical Chemistry C, 2012. 116(15): p. 8844-8848. Copyright 2012 American Chemical Society.

The topic of five-fold symmetry in nanoparticles has created a very large field of interest by the scientific community. Marks has reported more than 60,000 papers in which the word nanoparticle appears[12]. If we narrow the search to papers containing the words decahedral and icosahedral more than 2,658 references appear. This clearly indicates the broad interest in this topic. Despite that extensive work, many problems remain. In this review we will describe some of the interesting topics to be examined. We will discuss the nanoparticles as a function of size because as the number of atoms in the nanoparticle increases the properties change.

2) The case of clusters with a small number of atoms (size <2.5nm)

A first case of interest is the clusters in which there is a small number of atoms. As a general criterion a cluster will not show plasmonic behavior. In other words, they can be considered as a superatom with a discrete energy level[13, 14]. The pioneering work of Farges on argon clusters[15] and the Borel group in metals[16, 17] showed that five-fold clusters can be produced in a molecular beam. In the last decade advances in synthesis methods resulted in a new field known as “atomically precise clusters” indicating the control in the number of atoms. Those cluster are stabilized by an organic molecule capping. Clusters often contain one or more kernels with five-fold symmetry. Examples of decahedral clusters are the experimental results for Au_{20}[18], Au_{103}, Au_{130}[19] and Au_{246}[20]. A selection of gold clusters is shown in **Figure 4**.

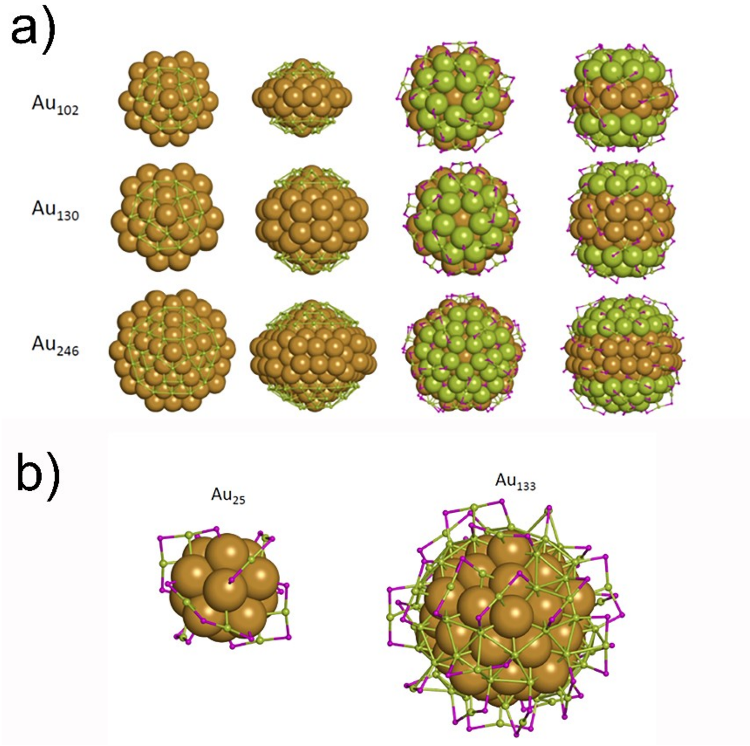

Figure 4: Here, several clusters of different atomic numbers are shown. In these clusters, there are areas that show five-fold symmetry.

In addition, Rossi and Ferrando have predicted a large number of poly-decahedral clusters[21]. Examples of icosahedral clusters are Au_{25} [22], Au_{144} [23] and several others. A remarkable cluster is the predicted icosahedral cluster Au_{60} [24, 25] which connects metals with fullerenes. In addition, several icosahedral cluster cages have been predicted[26, 27]. Finding those clusters experimentally is one of the most attractive challenges for researchers in this field.

It should be noted that in clusters the number of atoms on the surface is an important fraction of the total atoms. For Instance, in a one shell icosahedron 12 of the 13 atoms will be on the surface. In a 3-shell icosahedron of 147 atoms, 92 will be on the surface.

The latter cluster has a size of ~ 1.5 nm. In a 6-shell icosahedron of 923 atoms, 362 will be on the surface and will have a size of ~ 2.8 nm. The organic molecules on the surface bond strongly to the surface atoms and induce distortion which can propagate to the interior layers. Small strain can change the structure from FCC to decahedral. As noted by Bagley[28], if we assumed that each tetrahedron is distorted to a body centered orthorhombic lattice (BCO) all the tetrahedra will fit and no gap will be present. The lattice parameters of the BCO are a=1, b=1.37 and c=1.05 (in normalized units). This model was expanded by Yang[29] and Yacaman et al.[30,31] and appears to be plausible for very small clusters. Barnard and Chen[32] have shown that the decahedral and FCC shapes are equally likely for small nanoparticles, if a decahedral nucleus is very likely. During the growth of clusters an initial rapid coarsening stage is produced where there is no shape-selectivity, but during which shapes with a combination of (111)[33, 34] and (100) facets deviate from the geometric ideals. So, a shape distribution like the one shown in **Figure 4** will the most common case.

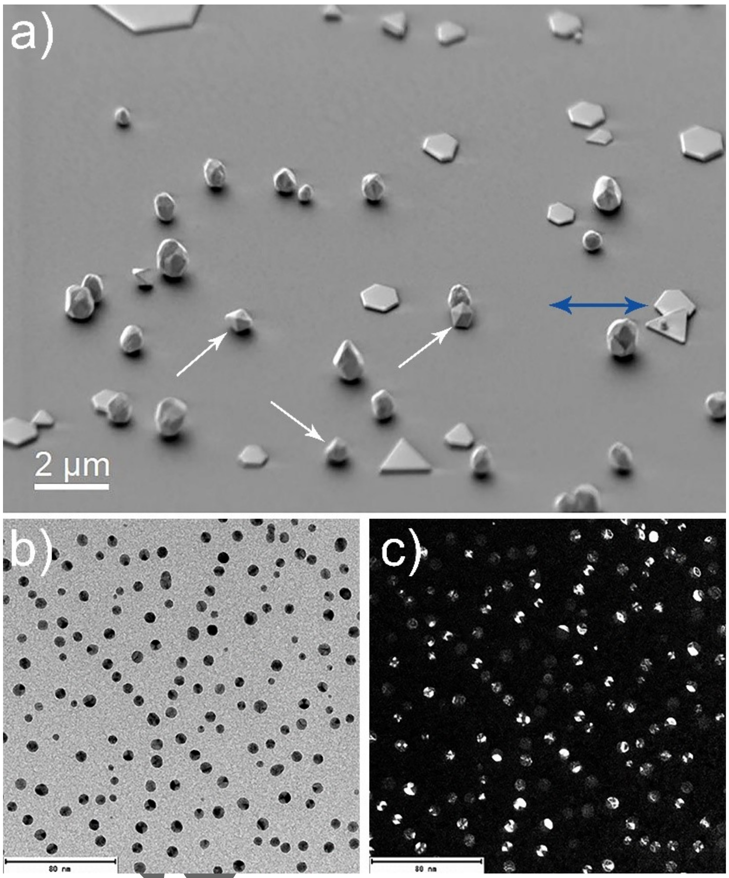

Figure 5: (a) SEM image showing the overall shape of micro-size particles. (b & c) Bright-field and dark-field images of Au nanoparticles. Dark-field imaging reveals their structure.

3) Nanoparticles with size >2.5 nm

The case of nanoparticles with a larger size is very different than that of clusters. As the size increases the atoms in the interior become increasingly important. New mechanisms emerge to control the shape and equilibrium of nanoparticles. At first glance we expect the rules of crystallography will fully dominate the growth. Decahedral and icosahedral gold nanoparticles were first reported by Ino and Ogawa[10] and Alpress and Sanders[35]. Several calculations indicate that the decahedral and icosahedral nanoparticles are not stable beyond 2-3 nm in size[36-39]. Nevertheless, when nanoparticles > 3 nm are prepared the decahedral and icosahedral shapes dominate. A typical sample of Au nanoparticles is shown in **Figure 5**. As can be seen, most nanoparticles have a decahedral shape (marked by arrows) or a polyhedral decahedron (double lines) or icosahedral (thick) arrow. A significant number are hexagonal or triangular platelets which are known to have twins parallel to the surface[40]. An examination of larger area shows that only 105 of the particles correspond to a non-twinned FCC structure. A similar result has been reported by Koga[41].

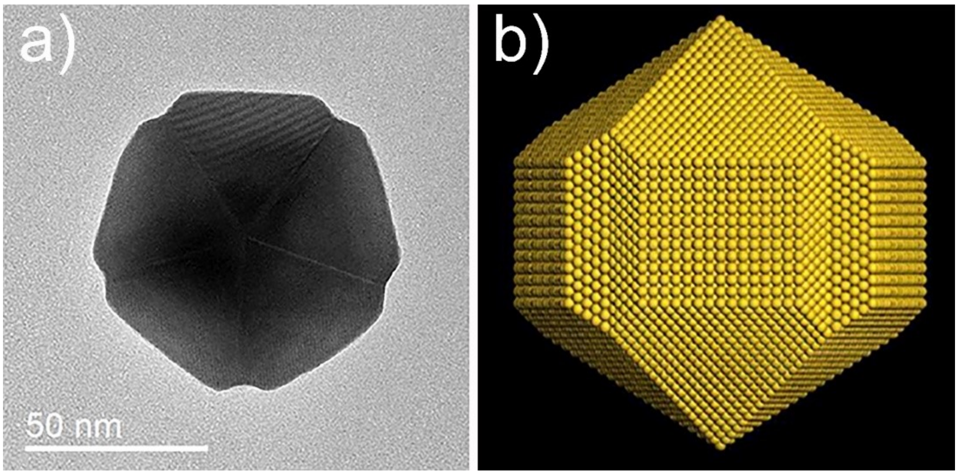

Figure 6: The Marks Decahedron showing the facets created in the particles. (a) Five-fold and (b) lateral views. Reprinted (adapted) with permission from Casillas et al., A New Mechanism of Stabilization of Large Decahedral Nanoparticles. Journal of Physical Chemistry C, 2012. 116(15): p. 8844-8848. Copyright 2012 American Chemical Society.

A question arises of how to explain the stability of five-fold symmetry in large particles. A first approach was reported by Ino[42] based on the minimization of the internal energy and application of the Wulff construction. This author predicted that (100) facets will develop into the decahedra. This structure is known as the Ino decahedra[40, 43].

A very important breakthrough was the work of Marks who introduced the twin boundaries contributions to the Gibbs free energy[44]. The result is that the particle will become faceted as shown in **Figure 6**. This structure was called "Marks Decahedron" by Landman[45, 46]. The name was widely accepted and is now a classical term in nanoparticles. The theoretical aspect of the Marks decahedron was later expanded by Patala et al[47]. Several other similar nanoparticle truncations have been reported in the literature for decahedral particles[41, 48] and for icosahedral particles[49]. The stability of the Marks Decahedron is remarkable. We perform some nanoparticle heating using electron irradiation. In **Figure 7**, we show a decahedral nanoparticle grown by evaporation on a substrate. The particle has straight facets and most likely was kinetically stabilized. After heating with the e-beam the nanoparticle becomes a Marks Decahedron (that indicates that the MD corresponds to a lower energy configuration. This supports the idea that twins and faceting introduce stability on the five-fold nanoparticles.

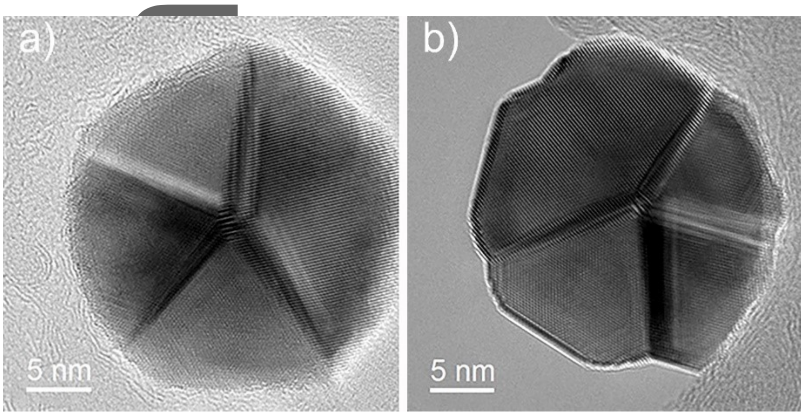

Figure 7: A particle grown on a substrate a) before electron heating. b) shows the particle after heating with the electron beam. The particle now shows facets and is a Marks Decahedron.

It has been established that twins are favored in nanocrystal growth[50, 51]. The so called WHS theory (Wagner, Hamilton and Seidensticker) predicts that twins in nanocrystals play the same role that dislocations do in bulk crystal growth. During the crystal growth, atoms arriving from the gas (or liquid phase) will be deposited to the lowest energy (111) facets.

However, the chances to nucleate a new layer (111) in the correct or incorrect registry are the same. Thus, a completely random stacking sequence of close packed layers, for example ...BCABACABA ...., would seem to be more favorable than either ...ABCABC... (fcc) or ...ABABAB... (hcp). This is not what is observed. In the WHS model, a single twin is introduced which favors nucleation in 4-coordinated sites. A nucleated island will spread over the two faces forming the reentrant corner until it reaches the extensions of the adjoining faces. This type of growth results in thin hexagonal platelets with well developed (111) faces, as the ones observed in **Figure 5**. Clearly, the reason for this is the absence of grooves and ridges on the (111) faces. In order to explain 3-growth it is necessary to assume a second twin lamella that intersects the (111) faces. This is the cross twin mechanism discovered by van der Waal[52]. Cross twinning leads directly to the formation of five-fold twins. Twins stabilize the nanoparticles, and along with surface faceting this might explain the prevalence of the five-fold shapes.

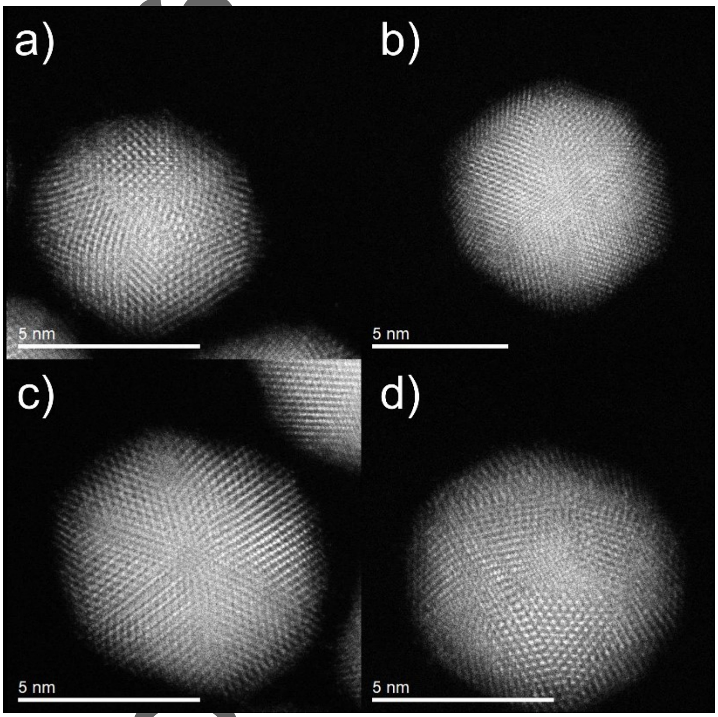

Figure 8: HAADF-STEM images of gold icosahedral nanoparticles in four different orientations. It can be observed that the near surface layers the atoms have a different stacking.

In addition, there is another possibility for growth of decahedral and icosahedral nanoparticles as reported by El Koraychy et al.[43] and Ma et al.[52] Decahedral and icosahedral nanoparticles can grow by coalescence of individual tetrahedra. This mechanism was first described by Balleto et al. for silver nanoclusters[53]. It is clear that for both mechanisms the decahedral and icosahedral particles are kinetically formed. Nevertheless, they are remarkably stable as we will show latter.

In the case of icosahedral particles an additional feature is observed in the layer stacking. As predicted by Settem and Kanjarla and Nelli and Ferrando[54, 55] the surface is reconstructed showing anti-Mackay stacking. We have systematically observed that in icosahedral particles the last few layers show a different stacking as shown in **Figure 8.** In the figure, four different nanoparticle orientations can be observed. In each case the near surface layers have a different stacking. In the icosahedral nanoparticles it is more difficult to obtain a low index plane that is aligned with the electron beam. Therefore, atomic resolution becomes more complicated to interpret. So, at this point we cannot fully corroborate that the stacking corresponds to anti-Mackay stacking. However, it seems difficult to explain the observed contrast with other mechanism. More research in this topic is needed.

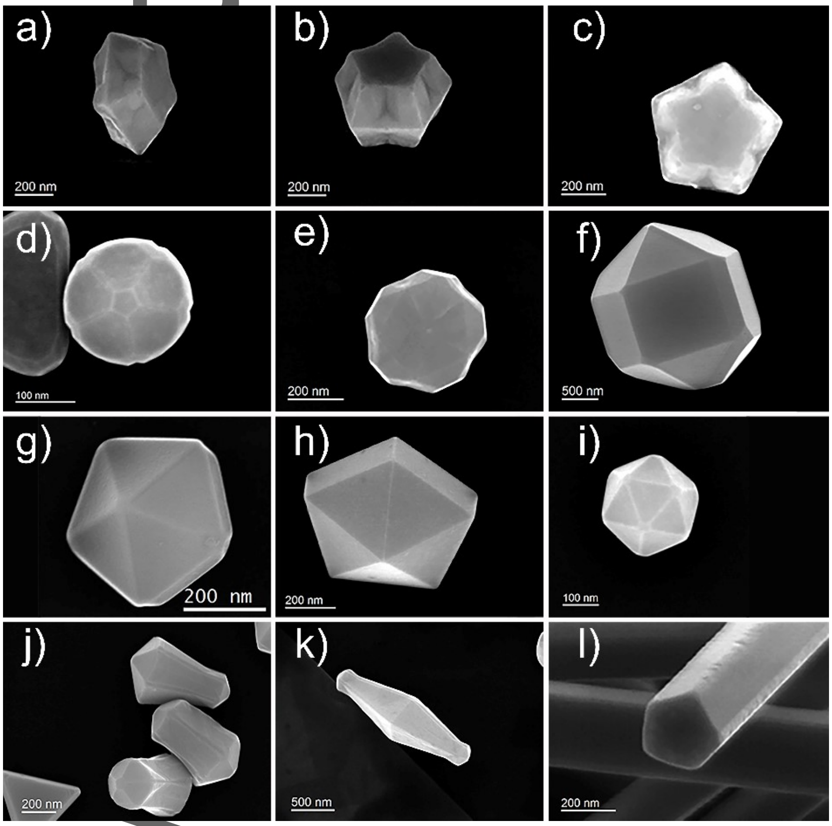

Figure 9: Various nanoparticles related to the decahedral and icosahedral shapes.

4) Nanoparticles with a size >100nm

As nanoparticles grow close to the micrometer range, several other polyhedral geometries begin to develop. A first group are the particles related to the decahedral and icosahedral geometry, some of these are shown in **Figure 9**. These structures include truncations of different types such as the Marks decahedron. However, there are additional geometries which produced shapes with even larger truncations. An interesting fact is that the Ino decahedra are observed frequently. If during the growth of the nanoparticle a surfactant is used to promote growth in a given direction, we see a myriad of elongated shapes which eventually lead to nanowires or nanorods. In the case of icosahedron, we can see the truncations described by Chui et al[56]. It should be mention that as demonstrated by Ma et al., decahedral and icosahedral nanoparticles can grow by coalescence of individual tetrahedra[57]. This can result in very large nanoparticles.

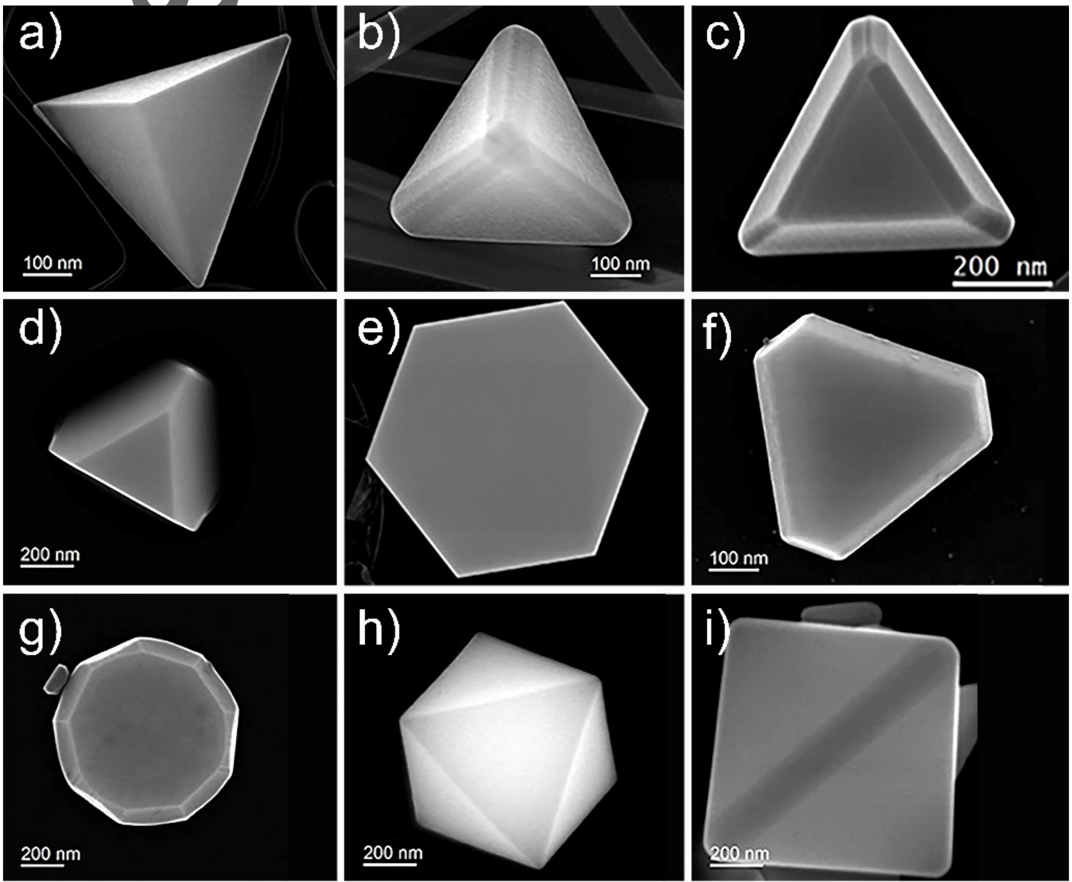

Figure 10: Micro-scale particles showing twin boundaries.

A second group of shapes are the ones corresponding to regular shapes shown in **Figure 10**. Most significant fact is that all the nanoparticles contain twins. An important portion of the observed nanoparticles have a hexagonal, triangular, tetrahedral, cubic and truncated platelets.

All these particles have a twin parallel to the surface[58]. When looking at the particles in **Figure 9**, **a), b),** and **h)** the twin are going through the particle. In **c)** through **g)**, the twin in along the edge of the particle. The twin is diagonal through the particle in the case of the cubic particle shown in **Figure 10 i)**, which is a twin across the (110) direction. In addition, we have different polyhedral such as: Trapezoid rhombic dodecahedron, truncated triakis icosahedron, the elongated pentagonal pyramid, the rhombicosidodecahedron and others which are part of the Johnson Solids. Those are shown in **Figure 11**. The growth of these shapes were discussed by Mariscal et al.[59] and Niu and Xu[60] who showed that Johnson solids can be expected for larger particles.

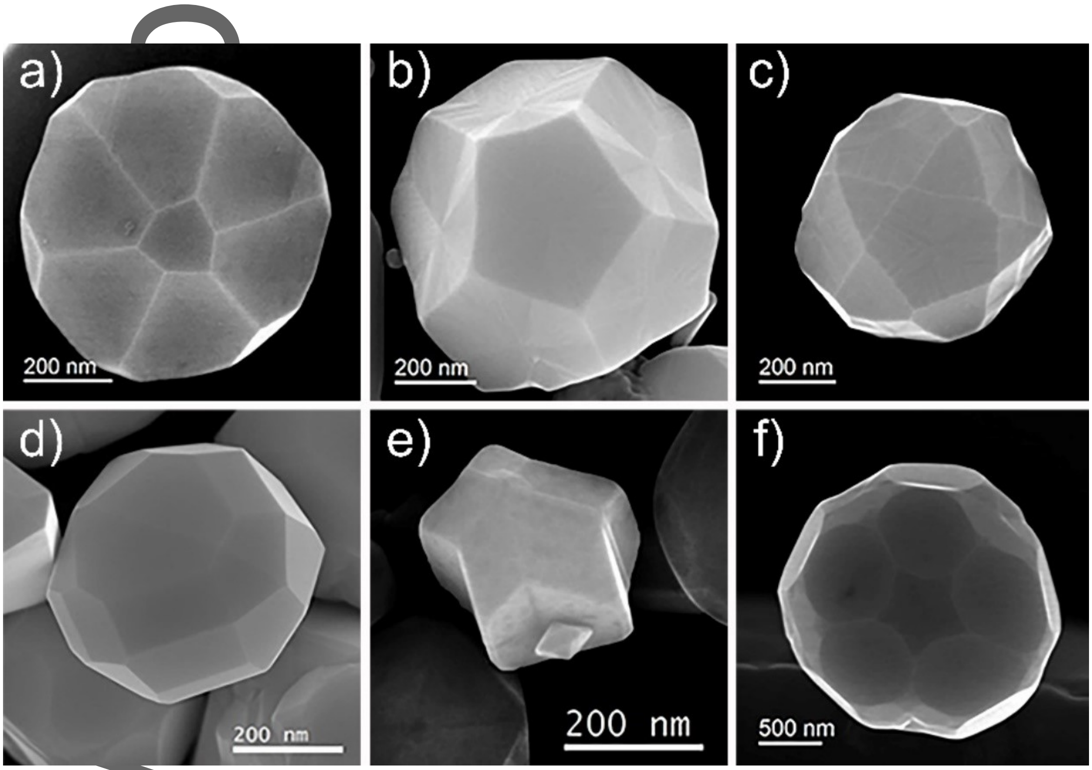

Figure 11: Various types of Johnson solids.

If during the particle growth, we add a surfactant, such as PVP, that will promote unidirectional growth in some lattice directions we end with elongated structures such as the silver nanowires[40] or gold nano stars[61-63]. Some of these shapes are shown in **Figure 12**.

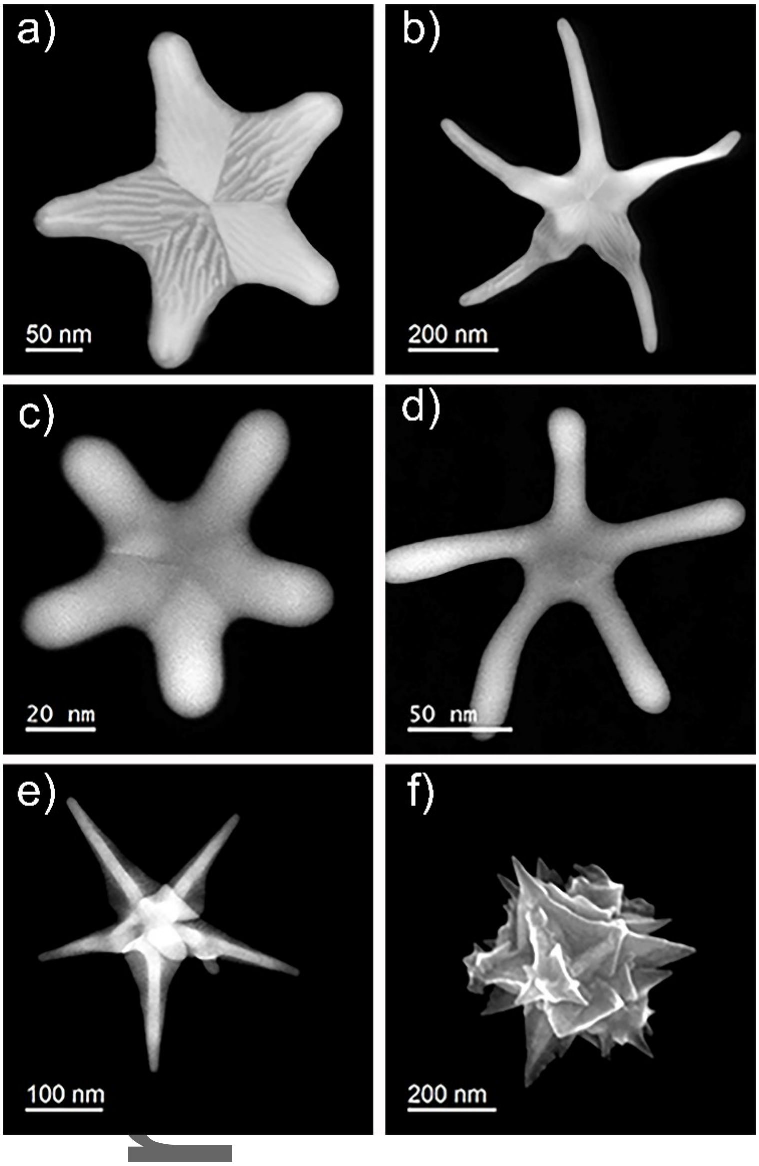

Figure 12: Different shapes can be obtained if during the growth process something is added to promote unidirectional growth.

Gold particles were synthesized via the polyol method using ethylene glycol (EG) and PVP (0.208g) in EG (5 mL) at 280^{o} C. The solution was withdrawn from the heat source and was cooled very rapidly in ice. Depending on the growth conditions, the particles can develop multiple faceting and the surface formation of a Zig-Zag faceting pattern as they get larger, this is shown in **Figure 13**.

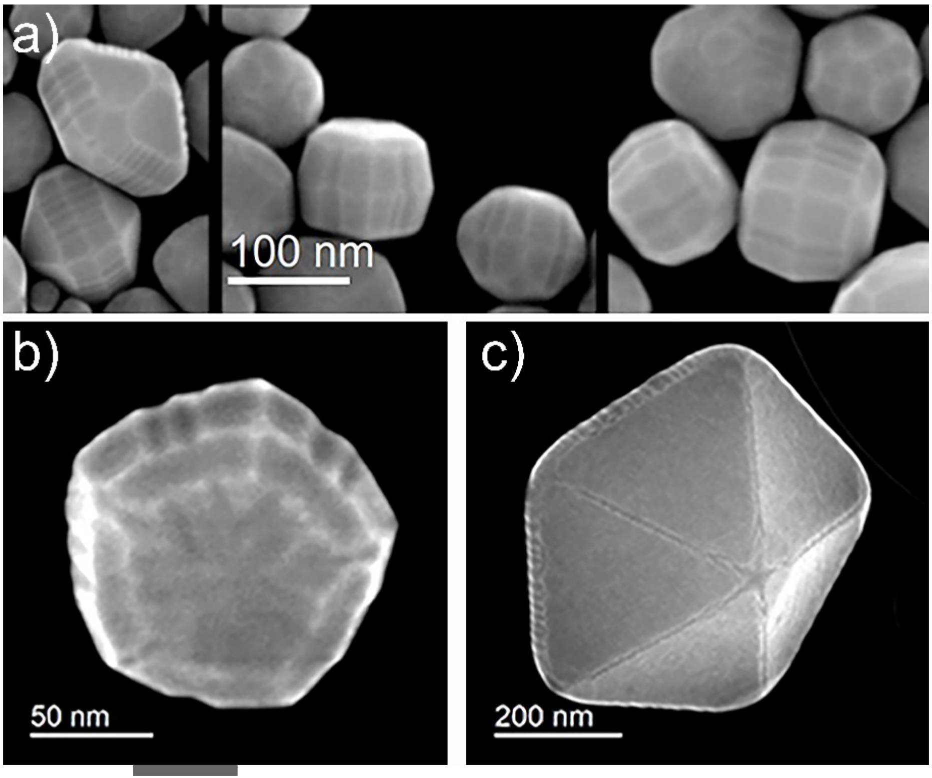

Figure 13: Gold nanoparticles that were cooled rapidly after synthesis in ice. The particles develop multiple facets and the formation of a Zig-Zag faceting pattern.

We were able to study some of these particles in an aberration corrected TEM. A decahedral particle was placed in such a way that the surface was perpendicular to the e-beam. The result is shown in **Figure 14** a) and b) which shows the decahedron at low magnification. HAADF images using an aberration corrected instrument shows that the corners are faceted as expected in a Marks decahedron (**Figure 14 c**). However, the surface between corners is formed by rounded promontories as shown in **Figure 14 d**). High magnification is seen in **Figure 14 e**). By using Cs-corrected STEM, it is possible to get atomic resolution imaging and determine the planes corresponding to these facets. The angle between the facets and the (001) planes is 14.8 degrees on average, while in a perfect crystal a (511) facet makes an angle of 15.79 degrees, with respect to a (001) plane. This is the best match; and the slight difference can be attributed to the rounded edges that connect the facets due to surface tension, as well as the internal strain existent in the lattice of the decahedron. The reason for this stability is that during synthesis fast cooling atoms of the nanoparticles do not have time to rearrange. This indicates that this is a kinetically driven shape. This is possible due to the stabilizing effect of the PVP; however, if removed, the facets will disappear. In this case, particles have rounded and smooth edges (**Figure 15**).

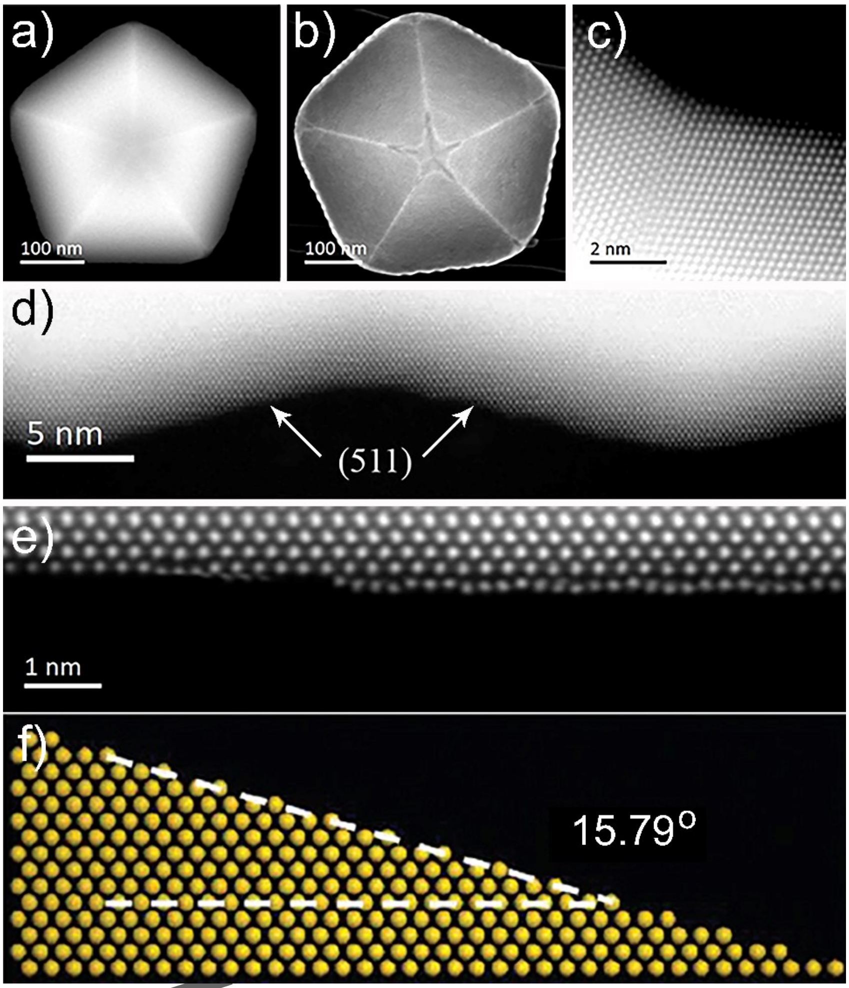

Figure 14: HAADF images of a gold nanoparticle that developed the zigzag pattern around the facet. The decahedral particle was oriented perpendicular to the e-beam. a) and b) show the decahedron at low mag. Marks decahedron (Figure 13 c). d) shows the corners are formed by rounded promontories. e) shows a high magnification of the edge of the particle. The angle between the facets and the (001) planes is 14.8-degree average while f) a perfect crystal (511) facet makes an angle of 15.79 degrees. Reprinted (adapted) with permission from Casillas et al., A New Mechanism of Stabilization of Large Decahedral Nanoparticles. Journal of Physical Chemistry C, 2012. 116(15): p. 8844-8848. Copyright 2012 American Chemical Society.

The result is a decahedron with no high index facets and very round contours at the twin boundaries. Hexagonal strings along the (110) orientation on the (001) terraces near the steps (**Figure 15b**) were observed, as well as strings along the (410) direction (**Figure 15c**). It has been proven that this reconstruction is more stable than the unreconstructed surfaces[64, 65]. This hexagonal reconstruction can take place by two different dislocations: dislocations formed by 5 and 3 columns of atoms. These types of dislocations, as described by Pao et al.[66] refer to the "arc" formed by 5 columns of atoms as a dislocation of type I and the one formed by 3 columns of atoms as a dislocation of type II. Both dislocations occur due to the insertion of an extra row of atoms to the (001) surface; however, they have different consequences in the stability of the surface. While type I dislocations increase the tensile strain, type II decrease it. On the other hand, they have the opposite effect on the surface energy, while type I dislocations decrease the surface energy, type II increase it. Formation of ridges and surface reconstruction is an additional factor to stabilize the nanoparticles as reported by Casillas et al[67].

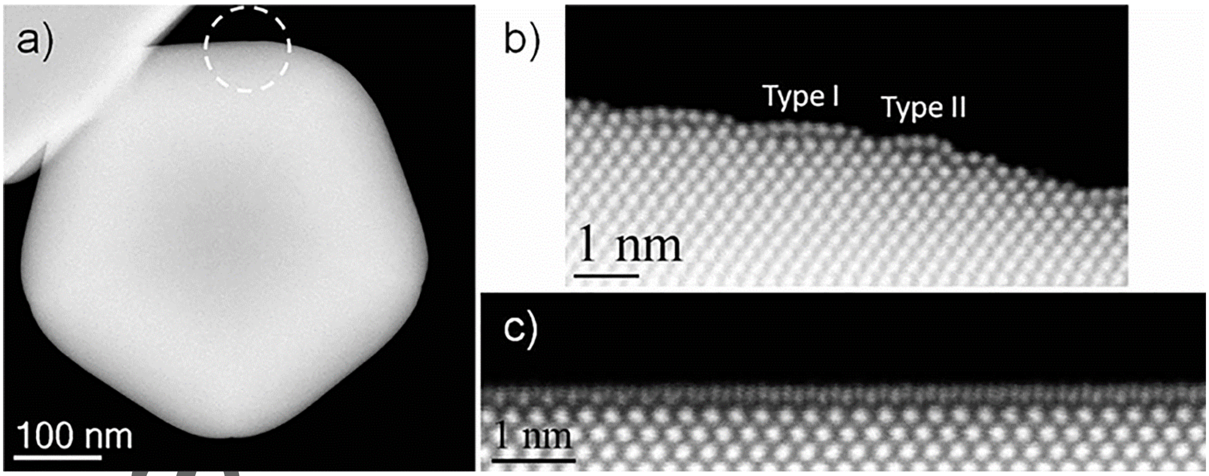

Figure 15: Showing a) a particle with rounded and smooth edges. b) shows hexagonal strings along the (110) orientation on the (001) terraces near the steps were observed, as well as c) strings along the (410) direction. Reprinted (adapted) with permission from Casillas et al., A New Mechanism of Stabilization of Large Decahedral Nanoparticles. Journal of Physical Chemistry C, 2012. 116(15): p. 8844-8848. Copyright 2012 American Chemical Society.

5) Strain in decahedral nanoparticles

It is expected that decahedral particles will have strain to close the gap, produced by the packing of regular FCC tetrahedra's we mention above. In the case of clusters, there is an easy pathway to a distortion from FCC-BCO. However, for larger particles, in which the role of the surface is reduced, it does not seem a likely mechanism. Homogeneous strain in decahedral structures was first introduced by Ino[42] and de Witt[68]. Later more sophisticated models were introduced by the group of Romanov[69-71]. Theoretical work by Patala et al[47, 72] demonstrated the role of strain in stabilizing the shape. Experimental reports on strain in decahedral nanoparticles are contradictory. On one hand, some works support homogeneous strain coupled with lattice bending[73]. On the other hand, some works support inhomogeneous strain[74].

To study this problem, we have used three different methods. The first one is the weak beam dark field method (WBDF). This method shows thickness fringes which can be used to study the shape of nanoparticles[9, 75]. The fringe contrast is also very sensitive to strain. In general fringes will be a superposition of thickness and bend contours. The use of Field Emission Gun Microscopes and CMOS cameras has allowed improved WBDF images. An example of WBDF images taking different diffraction spots to produce images of different sections of the decahedra, and these images are shown in **Figure 16**. The weak beam fringes are evenly spaced with a period equal to the extinction distance. However, if we measure the intensity variations along a thickness fringe, we can see intensity variations. Fringe space is modified by dynamical diffraction, however, variations of intensity along a fringe variation can only be due to strain. By tilting the sample in a slightly different direction we get the image of **Figure 16e**) in which stacking faults at the twin boundary are observed.

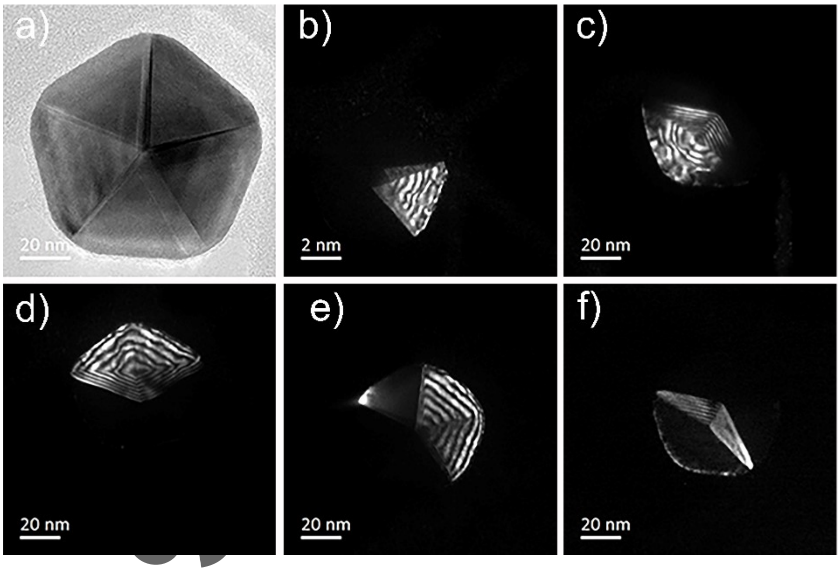

Figure 16: An example of Weak Beam Dark Field (WBDF) imaging. The weak beam fringes are evenly spaced with a period equal to the extinction distance. Fringe space is modified by dynamical diffraction, while variations in intensity along a fringe variation is due to strain. e) shows when the particle is tilted and the stacking faults at the twin boundary can be seen.

A second method is based on the analysis of a HAADF-STEM aberration corrected image. In this case the atomic columns on the image represent the true atomic positions. **Figure 17a**) shows a HAADF-STEM image of a decahedral particle. The FFT shows, **Figure 17b**), the overall five-fold symmetry (the pattern is indexed using FCC miller indexes). **Figure 17c)** shows the image formed using only the (111) spots and eliminating the rest. As can be seen, no strain distortion is present along the (111) planes. On the other hand, the image formed using only the spots of the (200) plane, Figure **17d)**, shows a very pronounced distortion. The center atomic array which is expected to be a perfect decahedron is heavily distorted.

A smaller particle is shown in **Figure 17e)** and **17f)** which is showing the same distortion. The incoherent twin boundaries are also apparent. The fact that the distortion appears only in the (200) planes was also reported by Peng et al[76]. A third method of measuring the strain is to apply the Geometrical Phase Analysis method[77, 78] to HAADF-STEM aberration corrected images. This method allows mapping of the strain on the image.

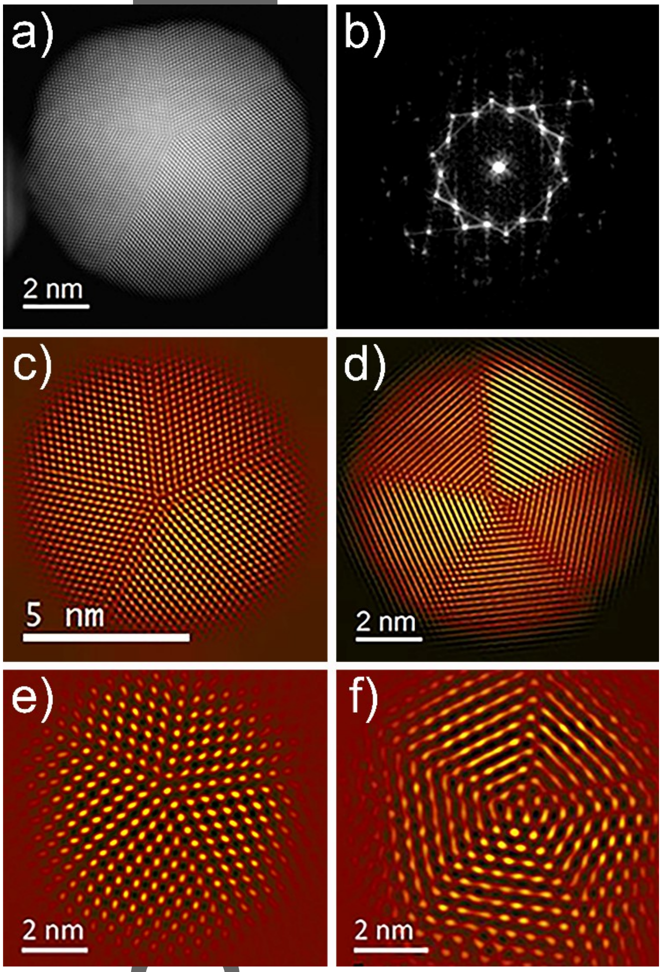

Figure 17: images. In this case the atomic columns on the image represent the true atomic positions. Figure 16a) shows a HAADF-STEM image of a decahedral particle. The FFT b) shows the overall five-fold symmetry. By showing only the spots corresponding to the (111) plan, c) no strain distortion is present. While looking at the (200) plane, d) there is a very pronounced distortion. The center atomic array which is expected to be a perfect decahedron is heavily distorted. In e) and f) a smaller particle is shown with the same distortion.

We have applied this method to decahedral particles. The result for the E_{xy} strain component is shown in **Figure 18** a) and b) for two different nanoparticles. As can be seen, the strain is concentrated along the twin boundaries and on the surface regions. Our findings confirm the findings of Johnson et al[74] and the theoretical predictions of Patala et al.[47] which is the fact that the strain distribution follows the 2+2+1 pattern. That means that strain is distributed with two pairs of tetrahedra with the same strain and one with a different pattern. We conclude that the strain distribution in five-fold nanoparticles is more complicated than expected and might even be different for two particles of the same shape and size.

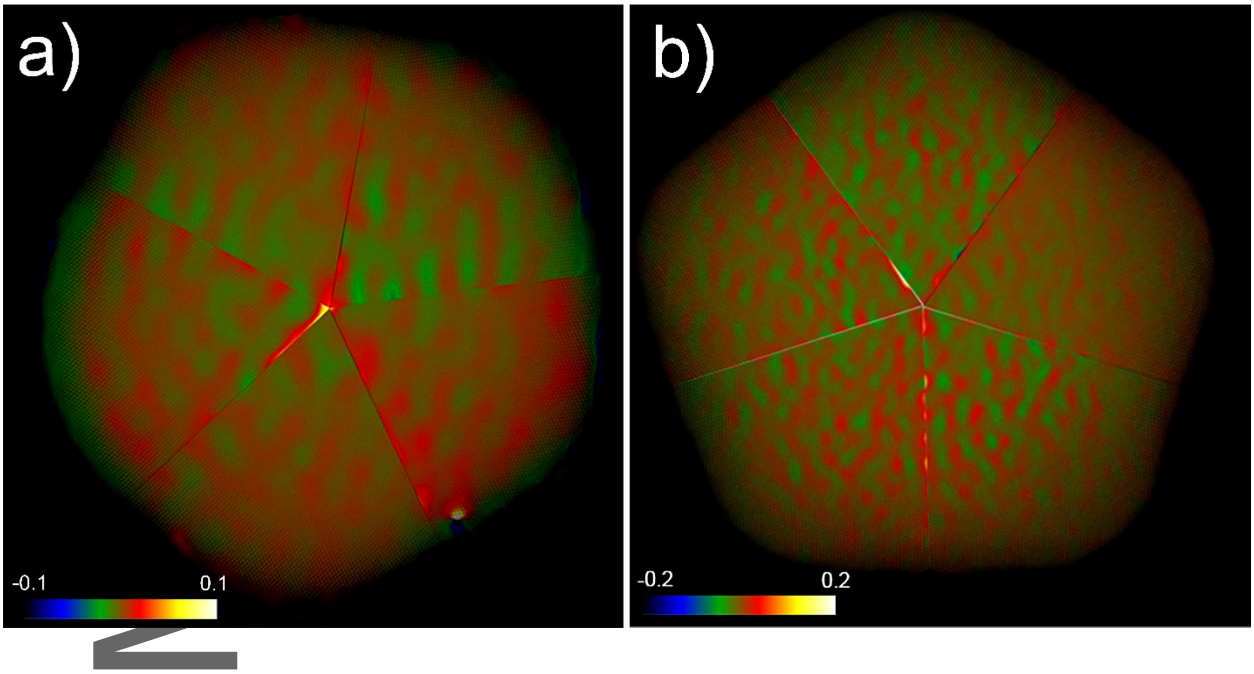

Figure 18: The result for the E_{xy} strain component is shown in a) and b) for two different nanoparticles. It can be seen that the strain is concentrated along the twin boundaries and along the surface regions.

6) Other Metals and multimetallic nanoparticles

So far, we have only discussed the case of Au, however, other metals show a similar behavior. Decahedral and icosahedral structures have been reported for Pd[79, 80], Cu[33], In[81], Ag[82], Ge[83] and others[84]. In many cases the nanoparticles are grown on substrates.

The possibility of having decahedral nanoparticles increases significantly when two metals are present. Decahedral and icosahedral particles have been reported for Fe-Pt[85], Pt-Pd[86], Pt-Co[87], Au-Co and many others[88]. The theory of bimetallic alloys has been extensively reported in literature[89-95]. It has been shown by Nelli et al.[94] that the evolution of bimetallic nanoparticles from initial core-shell configurations to their equilibrium intermixed chemical ordering arises from a complex interplay between interdiffusion of atoms and shape rearrangements. Normally in synthesizing bimetallic nanoparticles the method of producing a seed and then depositing the second metal is used[96]. This results in a core shell structure. Even when the precursor salts are simultaneously reduced, the rate of formation of metal atoms is different for each salt and this also results in a core-shell structure. We have studied the case of Au-Cu[97], Au-Pd[98], Au-Ag[99] and other alloys[88]. When the core seed is decahedral (or icosahedral) the shell follows that structure. Examples are shown in **Figure 19**. In a) and b) there is an Au-Cu core shell structure and its EDS analysis. In c) we show an Ag-Au core shell. It is very important to note than in this case the shell (Ag) has an FCC packing. The same packing is shown in the case of Pt-Pd, as shown in d).

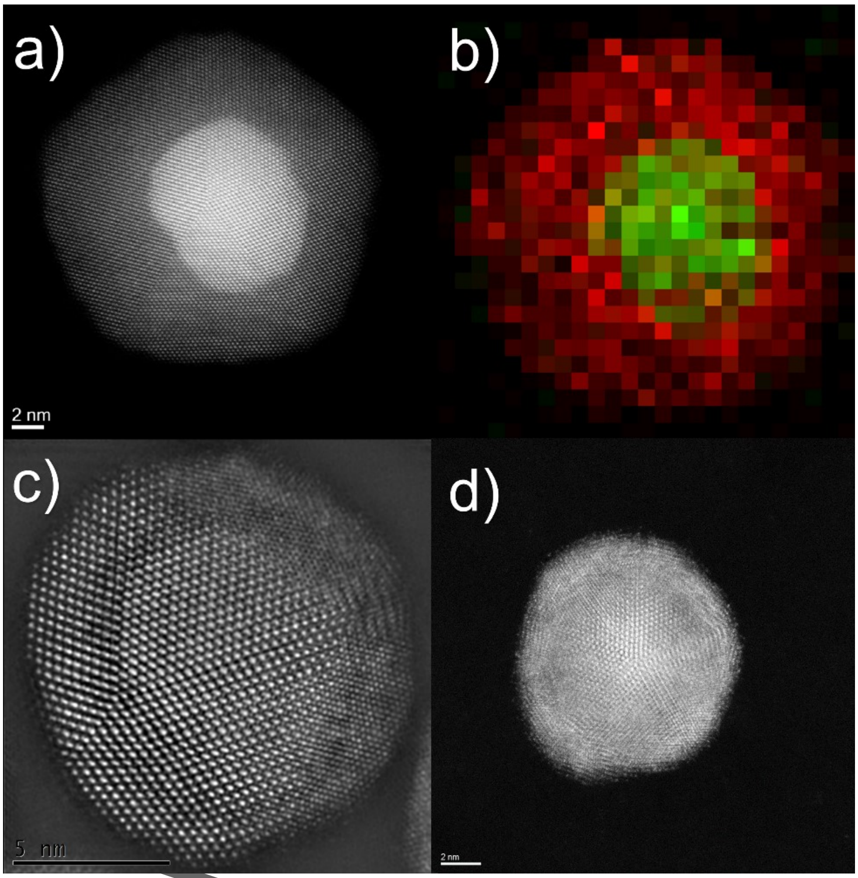

Figure 19: STEM-HAADF images of several bimetallic alloys. a) Au-Cu with the core and the shell have an overall decahedral shape. b) EDS map of the particle in a), red corresponds to Au and green to Cu. c) Au-Ag core shell. The Ag on the shell has a different packing than the Au core. d) Pt-Pd core shell, the overall particle is decahedral, but the Pt shell has a different packing.

When elements with different atomic radii are present in a nanoparticle the internal strain increases dramatically. The subsequent structure is the result of the strain engineering in nano alloys as described by Nelli et al. and Front et al[94, 100].

The strain increases with the number of elements on the alloy. The net result is that decahedral and icosahedral shapes become even more prominent. **Figure 20** shows examples of from a five-metal nanoparticle (Au/Cu/Pd/Ni/Cu) and a four-metal particle (Au/Cu/Co/Ni). Interestingly a core shell structure is formed with the decahedral core. The tendency to form core-shell is produced despite all the metal precursor salts are reduced simultaneously during the synthesis. In the case of multimetallic nanoparticles, the entropy makes a significant contribution to the Gibbs free energy. On the other hand, strain due to atomic radius differences becomes more significant. The particle shape will be determined by the minimization of the internal energy, including the contributions of strain and twins, and the maximization of entropy. At this point there are still many unknowns in this area, and it represents a big challenge for researchers on nanoparticle physics.

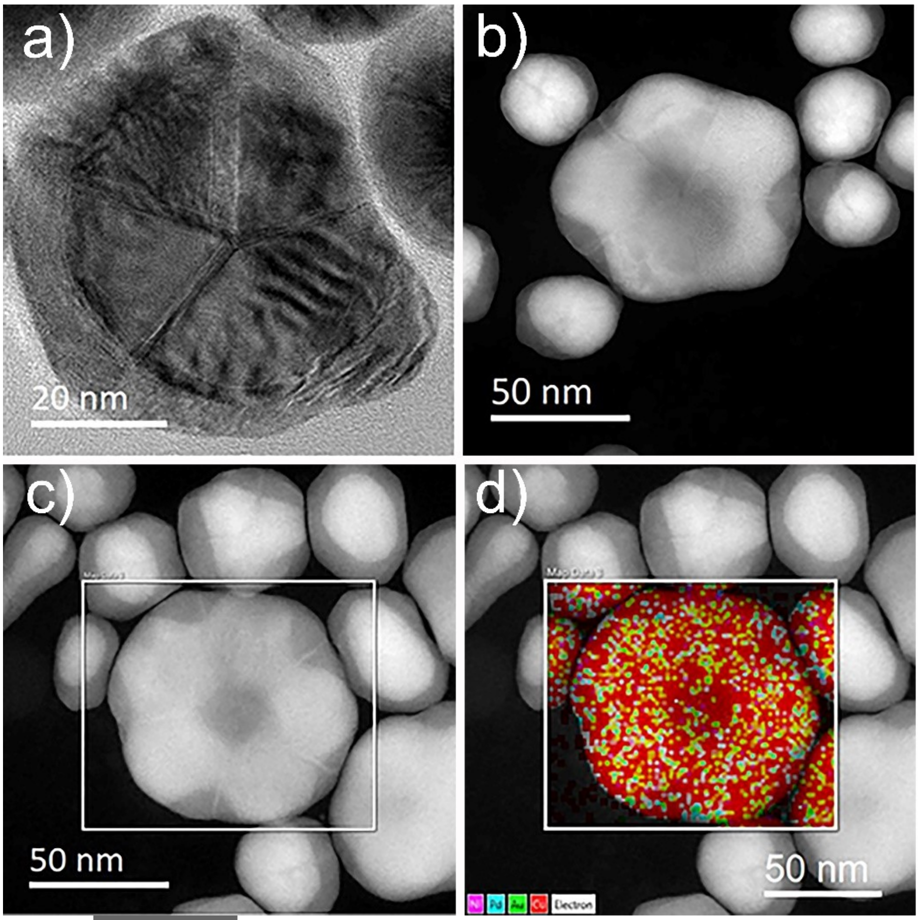

Figure 20: Here is an example of a five-metal a) nanoparticle Au/Cu/Pd/Ni/Cu and a four-metal b) particle Au/Cu/Co/Ni. It is interesting that a core shell structure is formed with the decahedral core.

7) Diffraction patterns of decahedral nanoparticles

Electron diffraction is a very powerful technique. It has become standard for researchers to use the FFT of a high-resolution micrograph as source of crystallographic data of nanoparticles. However, the FTT is not fully equal to the diffraction pattern and contains artifacts due the mathematical limitations. Electron diffraction contains more information specially about defects on structures. In recent years, the access of more coherent electron sources and aberration correction haves allowed the possibility of obtaining parallel beam diffraction with nanometric size[101-103]. These methods allow structural determination of nanoparticle facets[104]. We have applied nanobeam electron diffraction (or nano diffraction) to a decahedral particle. The whole particle shows overall five-fold symmetry. However, if we diffract individual tetrahedra, the patterns will resemble an FCC pattern in the (110) orientation. An example is shown in **Figure 21** a). The patterns were obtained avoiding the twin boundaries to avoid extra reflections. A similar figure for a Marks decahedron is shown in **Figure 21 b**). The results indicate that particles have a pseudo five-fold symmetry resulting from the superposition of individual diffraction patterns. However, if we examined a nanobeam patter obtained from the whole particle we can see that the angle between (111) spots changes between reflections as shown in **Figure 21 c**). As it can be seen in **Figure 21 c**) the angles follow a Zig-Zag pattern. The values of the larger and smaller angles are not exactly the same, but their summation equals 360°. Although the pattern in **Figure 21 c**) is slightly tilted away from the Laue condition, in which all the intensities are equal, the angular shift is far too long to be produced by tilting. The only possibility is strain produced to rotate the planes to close the gap. The (111) lattice orientation distances deviate from the bulk value by ± 0.16Å and again are different on every reflection because of the strain. A plot of the angles, due to the strain, of the diffraction pattern will be non-centrosymmetric as shown by Johnson et al[74]. This is consistent with the presence of phason distortion. Phasons are related to atomic displacements on the lattice and are commonly observed in non-periodic solids such as the quasicrystals[105]. One of the most characteristics of phason strain is the shift of diffraction spots in a zigzag along a line[106]. A possibility is that even though the individual tetrahedra are periodic crystals, the overall decagonal structure is not. Breaking the long-range periodicity on decahedral particles creates the conditions for phason distortion. The effect observed in diffraction patterns of decahedral particles as shown in **Figure 21**. It will be difficult to understand this effect without phason strain. However, this is again a topic that needs further research.

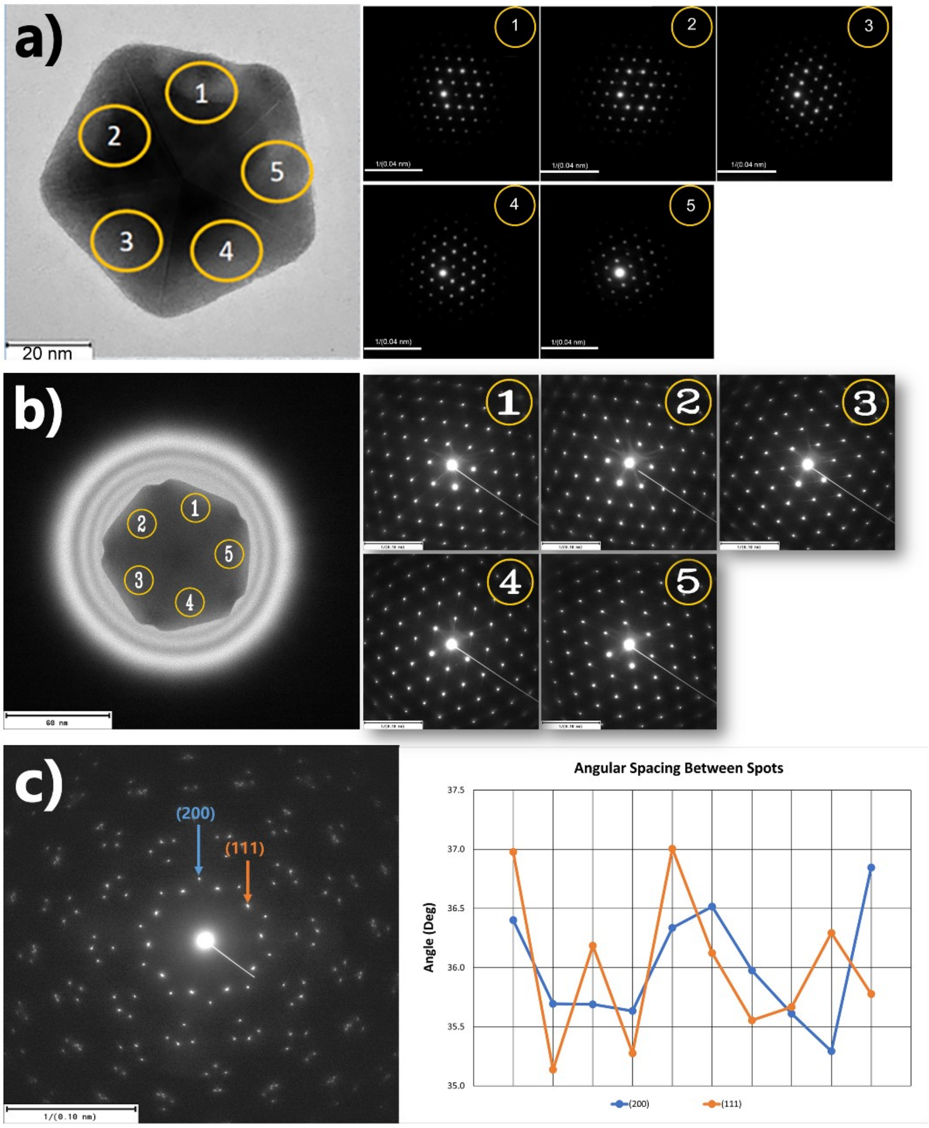

Figure 21: Nano diffraction of a) an individual tetrahedra nanoparticle. The pattern from the whole particle is shown along with the patterns for the individual areas that resemble (110) FCC patterns; b) a Marks decahedron with the corresponding diffraction patterns. c) shows the diffraction pattern of the tetrahedra nanoparticle showing the (111) and (200) diffraction spots. The plot shows that the angle between the spots has a zigzag pattern.

8) Influence of the preparation method

The way nanoparticles are synthesized has a great influence on the resulting shape. In this review we did not discuss this at length. There are plenty of examples on the literature that report changes on shape with the synthesis method[96, 107, 108]. We refer the reader to those papers. At the ends it is play between kinetics and thermodynamics that control the shapes discussed in references[12, 43, 59]. A very significant example is the growth of Ag nanowires. These are by adding a surfactant that produces preferential growth in one direction. Other methods include the polyol method and the use of a soft template[109, 110]. Nanowires have a decahedral structure that can be produced by a chain aggregation of single decahedra as reported by Reyes Gasga et al.[40]

9) Discussion and Conclusions

The decahedral and icosahedral are a fascinating subject. These structures are formed in several metals and in multimetallic nanoparticles. Decahedral nanoparticles can be produced by either growth of an initial decahedral nuclei or by coalescence of tetrahedral nanoparticles. In both cases these structures are kinetically stabilized, and it will be expected that if thermodynamic equilibrium is achieved, they will transform to FCC structures similar to the bulk. Nevertheless, decahedral and icosahedral nanoparticles are remarkably stable.

In SI section we show three videos of heating decahedral nanoparticles. In the video SI-1 we show a decahedral nanoparticle of 1.5 nm which is heated by a high dose electron beam. This corresponds to the phenomenon named quasimelting[111, 112]. The electron beam increases the nanoparticle temperature[34, 113] in a way proportional to its size. The particle is distorted but its shape remains overall decahedral. In the video SI-2 a particle of ~2.5 nm is shown, again the same trend is observed. A third example (also electron beam heating) of a larger decahedral particle ~3.5 nm is shown, which, despite the fluctuations remains decahedral. In SI-3 we show a sequence of heating of a large particle ~400 nm. In this case the heating was done in the TEM using a heating stage. The particle remains stable until 600ºC in which it is partially evaporated. The conclusion is that the decahedral nanoparticles are exceptionally stable. The cross-twinning mechanism appears to be the most significant in the growth of decahedral (and icosahedral) nanoparticles. Once formed, twins are very stable and they contribute to the internal energy. As the particle grows, the twin boundaries contribute more to the internal energy.

The twin's movement is not very likely unless a stress is applied to the nanoparticle. Full dislocations are not likely to formed and partial dislocations will tend to move to the twin boundaries. This situation is increased when there is more than one metal because there is strain due to differences on the lattice parameter. So even that these nanoparticles are kinetically formed, and they remain stable. The more metals the more likely that five-fold structures will be formed.

In addition, in monometallic systems the strain plays a role in the stability. There is not a single route to produce strain but rather a diversity of possibilities. As we have shown, two decahedral particles of the same size might have different stress profile and different defects.

In this paper we have presented most of the results for the case of Au. However, several other metals (and semiconductors and oxides) show decahedral and icosahedral structures. More research is needed to explore all the metals in the periodic table. As the size grows, new shapes are formed which are, in most cases, related to five-fold symmetry such as the truncated triakis Icosahedron and the rhombicosidodecahedron. In addition, as the nanoparticle grows faceting and surface reconstruction appears which further helps to stabilize the decahedral shape. The preparation method is also important in producing five-fold structures. That includes the synthesis temperature and the cooling method.

However, macroscopic single metal crystal with decahedral shape have not been observed. We have reported decahedral structures in Au with a size up to 1μm. Only in the case of quasicrystals have people been able to grow single crystals with five-fold symmetry; they always are formed by several metals. We have to assume that at one point of the growth there should be a transition from decahedral to the bulk structure of FCC. The mechanism of this transition is not known. No doubt that this is a topic which deserves attention from researchers and is part of the fascination of five-fold structures.

Author Contributions

RMC, AL, BR, DBU and LBD contributed with TEM experiments, analysis of data and paper editing. JVS contributed with synthesis of nanoparticles, analysis of data and editing; RW contributed to the analysis of data. MJY coordinated the work, contributed to data analysis and editing.

Conflicts of interest

There are no conflicts to declare.

Acknowledgements

The authors acknowledge the support of the Department of Energy grant Mission DAC: Molecular Mechanisms of Moisture Driven DAC with Charged Polymers. We thank the DOD for financial support of AL through the SMART scholarship program. RMC acknowledges the support of PAPIIT-UNAM grant IA102021 and J. Romero for technical assistance at LUME@IIM-UNAM. We also acknowledge the support from the ¡MIRA! NAU institute and the Arizona Board of Regents for support though the TRIFF program. MJY also wants to thank all the contributions, ideas and criticisms that were made during more than 25 years.

Uncategorized References

1. Hargittai, I., *Structures beyond crystals.* Journal of Molecular Structure, 2010. **976**(1-3): p. 81-86.
2. Gratias, D. and M. Quiquandon, *Discovery of quasicrystals: The early days.* Comptes Rendus Physique, 2019. **20**(7-8): p. 803-816.
3. Hofmeister, H., *Forty years study of fivefold twinned structures in small particles and thin films.* Crystal Research and Technology, 1998. **33**(1): p. 3-25.
4. Kroto, H., *Symmetry, space, stars, and C-60 (Nobel lecture).* Angewandte Chemie-International Edition, 1997. **36**(15): p. 1579-1593.
5. Jana, A.K. and E.R. May, *Structural and dynamic asymmetry in icosahedrally symmetric virus capsids.* Current Opinion in Virology, 2020. **45**: p. 8-16.
6. Douglas, T. and Y. Wang, *Bioinspired Approaches to Self-Assembly of Virus-like Particles: From Molecules to Materials.* Accounts of Chemical Research, 2022. **55**(10): p. 1349-1359.
7. Jose, J. and S.L. Hafenstein, *Asymmetry in icosahedral viruses.* Current Opinion in Virology, 2022. **54**.
8. Yacaman, M.J., K. Heinemann, and H. Poppa, *THE DETERMINATION OF THE HABIT PLANES OF NANOMETER-SIZE SINGLE-CRYSTAL GOLD PARTICLES.* Crc Critical Reviews in Solid State and Materials Sciences, 1981. **10**(3): p. 243-260.
9. Yacaman, M.J. and T. Ocanaz, *HIGH-RESOLUTION TOPOGRAPHICAL IMAGES OF SMALL METAL PARTICLES.* Applied Physics Letters, 1977. **30**(7): p. 359-360.
10. Ino, S. and S. Ogawa, *MULTIPLY TWINNED PARTICLES AT EARLIER STAGES OF GOLD FILM FORMATION ON ALKALIHALIDE CRYSTALS.* Journal of the Physical Society of Japan, 1967. **22**(6): p. 1365-&.
11. Marks, L.D., *EXPERIMENTAL STUDIES OF SMALL-PARTICLE STRUCTURES.* Reports on Progress in Physics, 1994. **57**(6): p. 603-649.
12. Marks, L.D. and L. Peng, *Nanoparticle shape, thermodynamics and kinetics.* Journal of Physics-Condensed Matter, 2016. **28**(5).
13. Aikens, C.M., *Electronic Structure of Ligand-Passivated Gold and Silver Nanoclusters.* Journal of Physical Chemistry Letters, 2011. **2**(2): p. 99-104.
14. Aikens, C.M., *Electronic and Geometric Structure, Optical Properties, and Excited State Behavior in Atomically Precise Thiolate-Stabilized Noble Metal Nanoclusters.* Accounts of Chemical Research, 2018. **51**(12): p. 3065-3073.

15. Farges, J., et al., *NONCRYSTALLINE STRUCTURE OF ARGON CLUSTERS .1. POLYICOSAHEDRAL STRUCTURE OF ARN CLUSTERS, 20 LESS-THAN N LESS-THAN 50.* Journal of Chemical Physics, 1983. **78**(8): p. 5067-5080.
16. Hall, B.D., et al., *AN ELECTRON-DIFFRACTION APPARATUS FOR STUDIES ON SMALL PARTICLES IN A MOLECULAR-BEAM.* Review of Scientific Instruments, 1991. **62**(6): p. 1481-1488.
17. Hall, B.D., et al., *MULTIPLY TWINNED STRUCTURES IN UNSUPPORTED ULTRAFINE SILVER PARTICLES OBSERVED BY ELECTRON-DIFFRACTION.* Physical Review B, 1991. **43**(5): p. 3906-3917.
18. Chen, J., et al., *Synthesis and Structure Determination of a New Au-20 Nanocluster Protected by Tripodal Tetraphosphine Ligands.* Inorganic Chemistry, 2014. **53**(8): p. 3932-3934.
19. Sakthivel, N.A. and A. Dass, *Aromatic Thiolate-Protected Series of Gold Nanomolecules and a Contrary Structural Trend in Size Evolution.* Accounts of Chemical Research, 2018. **51**(8): p. 1774-1783.
20. Vergara, S., et al., *MicroED Structure of Au-146(p-MBA)(57) at Subatomic Resolution Reveals a Twinned FCC Cluster.* Journal of Physical Chemistry Letters, 2017. **8**(22): p. 5523-5530.
21. Rossi, G. and R. Ferrando, *Freezing of gold nanoclusters into poly-decahedral structures.* Nanotechnology, 2007. **18**(22).
22. Zhu, M., et al., *Correlating the crystal structure of A thiol-protected Au-25 cluster and optical properties.* Journal of the American Chemical Society, 2008. **130**(18): p. 5883-+.
23. Yan, N., et al., *Unraveling the long-pursued Au144 structure by x-ray crystallography.* Science Advances, 2018. **4**(10).
24. Whetten, R.L., et al., *Chiral-Icosahedral (I) Symmetry in Ubiquitous Metallic Cluster Compounds (145A,60X): Structure and Bonding Principles.* Accounts of Chemical Research, 2019. **52**(1): p. 34-43.
25. Mullins, S.M., et al., *Chiral symmetry breaking yields the I-Au-60 perfect golden shell of singular rigidity.* Nature Communications, 2018. **9**.
26. Trombach, L., et al., *Hollow Gold Cages and Their Topological Relationship to Dual Fullerenes.* Chemistry-a European Journal, 2016. **22**(26): p. 8823-8834.
27. Ning, H., et al., *A series of quasi-icosahedral gold fullerene cages: Structures and stability.* Journal of Physics and Chemistry of Solids, 2014. **75**(5): p. 696-699.
28. Bagley, B.G., Nature, 1965. **208**.
29. Yang, C.Y., *CRYSTALLOGRAPHY OF DECAHEDRAL AND ICOSAHEDRAL PARTICLES .1. GEOMETRY OF TWINNING.* Journal of Crystal Growth, 1979. **47**(2): p. 274-282.
30. Yacaman, M.J., et al., *STRUCTURE OF SMALL, VAPOR-DEPOSITED PARTICLES .2. EXPERIMENTAL-STUDY OF PARTICLES WITH HEXAGONAL PROFILE.* Journal of Crystal Growth, 1979. **47**(2): p. 187-195.
31. Schabesretchkiman, P., et al., *MICRODIFFRACTION AND LATTICE RESOLUTION STUDIES OF FIVEFOLD SYMMETRY GOLD PARTICLES.* Journal of Vacuum Science & Technology A, 1984. **2**(1): p. 22-28.
32. Barnard, A.S. and Y. Chen, *Kinetic modelling of the shape-dependent evolution of faceted gold nanoparticles.* Journal of Materials Chemistry, 2011. **21**(33): p. 12239-12245.
33. Bhattacharjee, C.R., D.D. Purkayastha, and N. Das, *Surfactant-mediated low-temperature synthesis of phase pure multiply twinned copper nanoparticles under non-inert condition via thermal decomposition of copper malonate.* Materials Letters, 2013. **94**: p. 108-111.
34. Williams, P., *MOTION OF SMALL GOLD CLUSTERS IN THE ELECTRON-MICROSCOPE.* Applied Physics Letters, 1987. **50**(24): p. 1760-1762.
35. Allpress, J.G. and J.V. Sanders, *STRUCTURE AND ORIENTATION OF CRYSTALS IN DEPOSITS OF METALS ON MICA.* Surface Science, 1967. **7**(1): p. 1-&.
36. Ferrando, R., *Determining the equilibrium structures of nanoalloys by computational methods.* Journal of Nanoparticle Research, 2018. **20**(7).

37. Baletto, F. and R. Ferrando, *Structural properties of nanoclusters: Energetic, thermodynamic, and kinetic effects.* Reviews of Modern Physics, 2005. **77**(1): p. 371-423.
38. Barnard, A.S., *Modelling of nanoparticles: approaches to morphology and evolution.* Reports on Progress in Physics, 2010. **73**(8).
39. Barnard, A.S., *Direct Comparison of Kinetic and Thermodynamic Influences on Gold Nanomorphology.* Accounts of Chemical Research, 2012. **45**(10): p. 1688-1697.
40. Reyes-Gasga, J., et al., *On the structure of nanorods and nanowires with pentagonal cross-sections.* Journal of Crystal Growth, 2006. **286**(1): p. 162-172.
41. Koga, K., *Novel bidecahedral morphology in gold nanoparticles frozen from liquid.* Physical Review Letters, 2006. **96**(11).
42. Ino, S., *STABILITY OF MULTIPLY-TWINNED PARTICLES.* Journal of the Physical Society of Japan, 1969. **27**(4): p. 941-&.
43. El Koraychy, E., et al., *Growth mechanisms from tetrahedral seeds to multiply twinned Au nanoparticles revealed by atomistic simulations.* Nanoscale Horizons, 2022. **7**(8).
44. Marks, L.D., *MODIFIED WULFF CONSTRUCTIONS FOR TWINNED PARTICLES.* Journal of Crystal Growth, 1983. **61**(3): p. 556-566.
45. Cleveland, C.L. and U. Landman, *THE ENERGETICS AND STRUCTURE OF NICKEL CLUSTERS - SIZE DEPENDENCE.* Journal of Chemical Physics, 1991. **94**(11): p. 7376-7396.
46. Cleveland, C.L., et al., *Structural evolution of smaller gold nanocrystals: The truncated decahedral motif.* Physical Review Letters, 1997. **79**(10): p. 1873-1876.
47. Patala, S., L.D. Marks, and M.O. de la Cruz, *Thermodynamic Analysis of Multiply Twinned Particles: Surface Stress Effects.* Journal of Physical Chemistry Letters, 2013. **4**(18): p. 3089-3094.
48. Rodriguez-Lopez, J.L., et al., *Surface reconstruction and decahedral structure of bimetallic nanoparticles.* Physical Review Letters, 2004. **92**(19).
49. Chui, Y.H., et al., *Topological characterization of crystallization of gold nanoclusters.* Journal of Chemical Physics, 2006. **125**(11).
50. Wagner, R.S., *ON THE GROWTH OF GERMANIUM DENDRITES.* Acta Metallurgica, 1960. **8**(1): p. 57-60.
51. Hamilton, D.R. and R.G. Seidensticker, *PROPAGATION MECHANISM OF GERMANIUM DENDRITES.* Journal of Applied Physics, 1960. **31**(7): p. 1165-1168.
52. vandeWaal, B.W., *Cross-twinning model of fcc crystal growth.* Journal of Crystal Growth, 1996. **158**(1-2): p. 153-165.
53. Baletto, F., et al., *Dynamical effects in the formation of magic cluster structures.* Physical Review B, 2004. **69**(23).
54. Panizon, E. and R. Ferrando, *Strain-induced restructuring of the surface in core@shell nanoalloys.* Nanoscale, 2016. **8**(35): p. 15911-15919.
55. Settem, M. and A.K. Kanjarla, *Role of core-shell energetics on anti-Mackay, chiral stacking in AgCu nanoalloys and thermally induced transition to chiral stacking.* Scientific Reports, 2020. **10**(1).
56. Chui, Y.H., et al., *Modeling the crystallization of gold nanoclusters-the effect of the potential energy function.* Journal of Physics-Condensed Matter, 2009. **21**(14).
57. Ma, X.M., et al., *Unveiling Growth Pathways of Multiply Twinned Gold Nanoparticles by In Situ Liquid Cell Transmission Electron Microscopy.* Acs Nano, 2020. **14**(8): p. 9594-9604.
58. Lee, J.W., et al., *Growth process of the ridge-trough faces of a twinned crystal.* Acta Crystallographica a-Foundation and Advances, 2005. **61**: p. 405-410.
59. Mariscal, M.M., J.J. Velazquez-Salazar, and M.J. Yacaman, *Growth mechanism of nanoparticles: theoretical calculations and experimental results.* Crystengcomm, 2012. **14**(2): p. 544-549.
60. Niu, W.X. and G.B. Xu, *Crystallographic control of noble metal nanocrystals.* Nano Today, 2011. **6**(3): p. 265-285.

61. Murphy, C.J., et al., *One-dimensional colloidal gold and silver nanostructures.* Inorganic Chemistry, 2006. **45**(19): p. 7544-7554.
62. Murphy, C.J., et al., *Surfactant-directed synthesis and optical properties of one-dimensional plasmonic metallic nanostructures.* Mrs Bulletin, 2005. **30**(5): p. 349-355.
63. Murphy, C.J., et al., *Gold nanorod crystal growth: From seed-mediated synthesis to nanoscale sculpting.* Current Opinion in Colloid & Interface Science, 2011. **16**(2): p. 128-134.
64. Zhang, K., Y. Zhang, and L. Shi, *A review of linear carbon chains.* Chinese Chemical Letters, 2020. **31**(7): p. 1746-1756.
65. Shi, H. and C. Stampfl, *Shape and surface structure of gold nanoparticles under oxidizing conditions.* Physical Review B, 2008. **77**(9): p. 094127.
66. Pao, C.-W., D.J. Srolovitz, and H.W. Zandbergen, *Thermodynamic and kinetic properties of surface dislocations on Au (001) from atomistic simulations.* Physical Review B, 2007. **75**(19): p. 195405.
67. Casillas, G., J.J. Velazquez-Salazar, and M. Jose-Yacaman, *A New Mechanism of Stabilization of Large Decahedral Nanoparticles.* Journal of Physical Chemistry C, 2012. **116**(15): p. 8844-8848.
68. Witt, D., *Partial dislocations* J of Physics C : solid state 1972. **64**: p. 529-534.
69. Romanov, A.E. and A.L. Kolesnikova, *Application of disclination concept to solid structures.* Progress in Materials Science, 2009. **54**(6): p. 740-769.
70. Romanov, A.E., et al., *VOIDS AND CHANNELS IN PENTAGONAL CRYSTALS.* Journal of Crystal Growth, 1993. **129**(3-4): p. 691-698.
71. Gryaznov, V.G., et al., *Pentagonal symmetry and disclinations in small particles.* Crystal Research and Technology, 1999. **34**(9): p. 1091-1119.
72. Patala, S., L.D. Marks, and M.O. de la Cruz, *Elastic Strain Energy Effects in Faceted Decahedral Nanoparticles.* Journal of Physical Chemistry C, 2013. **117**(3): p. 1485-1494.
73. Wu, H., et al., *Size-dependent strain in fivefold twins of gold.* Acta Crystallographica Section B-Structural Science Crystal Engineering and Materials, 2021. **77**: p. 93-98.
74. Johnson, C.L., et al., *Effects of elastic anisotropy on strain distributions in decahedral gold nanoparticles.* Nature Materials, 2008. **7**(2): p. 120-124.
75. Yacaman, M.J., *CHARACTERIZATION OF SUPPORTED CATALYSTS BY TRANSMISSION ELECTRON-MICROSCOPY.* Applied Catalysis, 1984. **13**(1): p. 1-25.
76. Peng, X.Y., et al., *Strain study of gold nanomaterials as HR-TEM calibration standard.* Micron, 2015. **79**: p. 46-52.
77. Hytch, M.J., E. Snoeck, and R. Kilaas, *Quantitative measurement of displacement and strain fields from HREM micrographs.* Ultramicroscopy, 1998. **74**(3): p. 131-146.
78. Hytch, M.J., J.L. Putaux, and J.M. Penisson, *Measurement of the displacement field of dislocations to 0.03 angstrom by electron microscopy.* Nature, 2003. **423**(6937): p. 270-273.
79. He, J.T., et al., *Controllable Synthesis of Marks Decahedral Pd Nanoparticles via Etching.* Journal of Nanoscience and Nanotechnology, 2018. **18**(12): p. 8276-8281.
80. Ji, W.H., et al., *Synthesis of Marks-Decahedral Pd Nanoparticles in Aqueous Solutions.* Particle & Particle Systems Characterization, 2014. **31**(8): p. 851-856.
81. Chen, Q., M. Tanaka, and K. Furuya, *Unusual crystallographic structure and its fluctuation of indium nanoparticles as-deposited and observed with HRTEM using the UHV-DC-TEM system.* Surface Science, 1999. **440**(3): p. 398-406.
82. Chen, Q., et al., *Polymer Driven Covalently Bonded Decahedral-Twinning of Ag Nanoparticles Prepared by ICP Enhanced Magnetron Sputtering Method.* Journal of Physical Chemistry C, 2009. **113**(18): p. 7633-7638.
83. Wu, Y., M. Takeguchi, and K. Furuya, *High resolution transmission electron microscopy study on the structure of Ge nanoparticles by using an ultrahigh vacuum-molecular beam epitaxy-transmission electron microscope system.* Japanese Journal of Applied Physics Part 1-Regular Papers Short Notes & Review Papers, 1999. **38**(12B): p. 7241-7246.

84. Zhou, S., et al., *Decahedral nanocrystals of noble metals: Synthesis, characterization, and applications.* Materials Today, 2019. **22**: p. 108-131.
85. Li, Z.A., et al., *Chemically ordered decahedral FePt nanocrystals observed by electron microscopy.* Physical Review B, 2014. **89**(16).
86. Paz-Borbon, L.O., A. Gupta, and R.L. Johnston, *Dependence of the structures and chemical ordering of Pd-Pt nanoalloys on potential parameters.* Journal of Materials Chemistry, 2008. **18**(35): p. 4154-4164.
87. Yang, Y., et al., *Structures, Thermal Stability, and Chemical Activity of Crown-Jewel-Structured Pd-Pt Nanoalloys.* Journal of Physical Chemistry C, 2015. **119**(20): p. 10888-10895.
88. Bhattarai, N., et al., *Structure and composition of Au/Co magneto-plasmonic nanoparticles.* Mrs Communications, 2013. **3**(3): p. 177-183.
89. Baletto, F., *Structural properties of sub-nanometer metallic clusters.* Journal of Physics-Condensed Matter, 2019. **31**(11).
90. Baletto, F. and R.L. Johnston, *Shaping nano-catalysts.* European Physical Journal B, 2019. **92**(7).
91. Calvo, F. and C. Mottet, *Order-disorder transition in Co-Pt nanoparticles: Coexistence, transition states, and finite-size effects.* Physical Review B, 2011. **84**(3).
92. Ferrando, R., *Nonequilibrium phenomena in nanoalloys: From nucleation to ageing*, in *Structure and Properties of Nanoalloys*. 2016. p. 185-228.
93. Ferrando, R., *Equilibrium structures of nanoalloys*, in *Structure and Properties of Nanoalloys*. 2016. p. 131-183.
94. Nelli, D., C. Mottet, and R. Ferrando, *Interplay between interdiffusion and shape transformations in nanoalloys evolving from core-shell to intermixed structures.* Faraday Discussions.
95. Pavan, L., K. Rossi, and F. Baletto, *Metallic nanoparticles meet metadynamics.* Journal of Chemical Physics, 2015. **143**(18).
96. Lohse, S.E. and C.J. Murphy, *The Quest for Shape Control: A History of Gold Nanorod Synthesis.* Chemistry of Materials, 2013. **25**(8): p. 1250-1261.
97. Guisbiers, G., et al., *Gold Copper Nano-Alloy, "Tumbaga", in the Era of Nano: Phase Diagram and Segregation.* Nano Letters, 2014. **14**(11): p. 6718-6726.
98. Bhattarai, N., et al., *Origin and shape evolution of core-shell nanoparticles in Au-Pd: from few atoms to high Miller index facets.* Journal of Nanoparticle Research, 2013. **15**(6).
99. Guisbiers, G., et al., *Electrum, the Gold-Silver Alloy, from the Bulk Scale to the Nanoscale: Synthesis, Properties, and Segregation Rules.* Acs Nano, 2016. **10**(1): p. 188-198.
100. Front, A. and C. Mottet, *Trends of chemical ordering in Pt-based nanoalloys.* Theoretical Chemistry Accounts, 2022. **141**(1).
101. Zuo, J., et al., *Quantitative electron diffraction and applications to materials science.* Microbeam Analysis, 1995: p. 269-270.
102. Zuo, J.M., *Electron Microscopy Techniques for Characterization of Nanomaterials.* Nanofabrication Towards Biomedical Applications: Techniques, Tools, Applications, and Impact, 2005: p. 135-162.
103. Zuo, J.M. and J.C. Spence, *Advanced transmission electron microscopy*. 2017: Springer.
104. Shah, A.B., et al., *High-index facets in gold nanocrystals elucidated by coherent electron diffraction.* Nano letters, 2013. **13**(4): p. 1840-1846.
105. Steurer, W., *Quasicrystals: What do we know? What do we want to know? What can we know?* Acta Crystallographica a-Foundation and Advances, 2018. **74**: p. 1-11.
106. Lubensky, T.C., et al., *Distortion and Peak Broadening in Quasicrystal Diffraction Patterns.* Physical Review Letters, 1986. **57**(12): p. 1440-1443.
107. Seo, D., et al., *Shape adjustment between multiply twinned and single-crystalline polyhedral gold nanocrystals: Decahedra, icosahedra, and truncated tetrahedra.* Journal of Physical Chemistry C, 2008. **112**(7): p. 2469-2475.

108. Hofmeister, H., *Shape variations and anisotropic growth of multiply twinned nanoparticles.* Zeitschrift Fur Kristallographie, 2009. **224**(11): p. 528-538.
109. Ha, H., et al., *Mini review of synthesis strategies of silver nanowires and their applications.* Colloid and Interface Science Communications, 2022. **50**.
110. Zhang, P., et al., *Silver nanowires: Synthesis technologies, growth mechanism and multifunctional applications.* Materials Science and Engineering B-Advanced Functional Solid-State Materials, 2017. **223**: p. 1-23.
111. Bovin, J.O., R. Wallenberg, and D.J. Smith, *IMAGING OF ATOMIC CLOUDS OUTSIDE THE SURFACES OF GOLD CRYSTALS BY ELECTROSCOPY.* Nature, 1985. **317**(6032): p. 47-49.
112. Dundurs, J., L.D. Marks, and P.M. Ajayan, *STRUCTURAL FLUCTUATIONS IN SMALL PARTICLES.* Philosophical Magazine a-Physics of Condensed Matter Structure Defects and Mechanical Properties, 1988. **57**(4): p. 605-620.
113. Gryaznov, V.G., A.M. Kaprelov, and A.Y. Belov, *REAL TEMPERATURE OF NANOPARTICLES IN ELECTRON-MICROSCOPE BEAMS.* Philosophical Magazine Letters, 1991. **63**(5): p. 275-279.

Five-fold symmetry is common in macroscopic nature; however, it is not seen in metallic crystals at the macroscopic scale. But, when looking at the nanoscale, metallic nanoparticles and nanoalloys exhibit decahedral and icosahedral pseudo five-fold symmetry. This is a review of gold and other metals alloyed in nanoparticles and the prevalence of five-fold symmetry.